Technical University of Denmark

DTU

Development of Refractory Ceramics for The Oxygen Evolution Reaction (OER) Electrocatalyst Support for Water Electrolysis at elevated temperatures

Nikiforov, Aleksey Valerievich; Prag, Carsten Brorson; Polonsky, J.; Petrushina, Irina; Christensen, Erik; Bjerrum, Niels J.

DTU Library
Technical Information Center of Denmark

Development of Refractory Ceramics for The Oxygen Evolution Reaction (OER) Electrocatalyst Support for Water Electrolysis at elevated temperatures.

A. V. Nikiforov[a], C. B. Prag[a], J. Polonský[b], I.M. Petrushina[a], E. Christensen[a] and N. J. Bjerrum[a]

[a] Energy and Materials Science Group, Department of Chemistry, Technical University of Denmark, Kemitorvet 207, DK-2800 Kgs. Lyngby, Denmark
[b] Department of Inorganic Technology, Faculty of Chemical Technology, Institute of Chemical Technology, Prague, Technická 5, 166 28 Praha 6-Dejvice, Czech Republic

Commercial TaC and Si_3N_4 powders were tested as possible electrocatalyst support materials for the Oxygen Evolution Reaction (OER) for PEM water electrolysers, operating at elevated temperatures. TaC and Si_3N_4 were characterised by thermogravimmetric and differential thermal analysis for their thermal stability. The Adams fusion method was implemented to deposit IrO_2 on the support surfaces. A series of electrocatalysts was prepared with a composition of $(IrO_2)_x(TaC/ Si_3N_4)_{1-x}$, where x represents the mass fraction of IrO_2 and was equal to 0.1 (only for TaC), 0.3, 0.5, 0.7, 0.9 and 1. The thin-film method was used for electrochemical analysis of the prepared electrocatalysts. SEM-EDX, BET and powder conductivity measurements were used as complementary techniques to complete characterisation of the electrocatalysts. Additionally, they were compared in their properties with previously reported data for a SiC-Si support. The stability of the electrocatalysts was assessed by estimation of reversibility of the anodic/cathodic processes.

Introduction

Currently, the only practically applicable anode electrocatalyst for the polymer electrolyte membrane water electrolysers (PEMWEs) is iridium oxide and it must be used at quite high loadings (about 1-2 mg/cm^2). Therefore, there is an obvious requirement to reduce the amount of used electrocatalyst to make the PEMWE devices economically viable. One of the options for reducing the loading is introduction of an electrocatalyst support. However, elevated temperatures (up to 200°C) in combination with acidic electrolytes limits the choice of possible materials for such systems (1). Ceramic powders present a class of potentially good candidates for the role of catalyst support. Previous work showed the successful implementation of SiC-Si powder as a support for active IrO_2 (1). In present work two other possible supports, namely TaC and Si_3N_4 are tested and their properties are compared with previously published data. As it was shown recently, these materials are stable in harsh environments, simulating those of the working electrolyser cell (2).

Electronic conductivity is an important parameter that influences electrocatalyst performance. One must consider the difference between the conductivity of the electrocatalyst support and of the entire composite material, consisting of the support and the active electrocatalyst layer on the surface. As the conductivity of unsupported IrO_2 is

sufficient for the operation of a PEMWE, it can be assumed to be sufficient in the case when IrO_2 covers most of the support, i.e. when it exceeds the percolation level. Consequently, even a non-conductive support may be acceptable for the application. Si_3N_4 is known as a poorly conductive material in contrast to TaC, which possesses electronic conductivity at a high level (3). Besides this, support powders investigated in this work had similar physical properties. Therefore, it was important to investigate their behaviour and development of physical properties with increasing portion of the IrO_2 in the prepared supported electrocatalysts.

Experimental

Electrocatalyst preparation

TaC, provided by Sigma-Aldrich, (99%) and Si_3N_4, provided by Goodfellow (> 85%) powders were introduced at the initial stage of the Adams fusion method of IrO_2 synthesis and supported electrocatalyst powders were prepared with varying content of IrO_2. The precursor $H_2IrCl_6 \cdot 4H_2O$ was provided by Alfa Aesar (99%) and was added to isopropanol and stirred for 1 hour to ensure complete dissolution of the salt. After the addition of grounded $NaNO_3$ (approximately in 20 times molar excess), the mixture was heated in air to 70 °C and evaporated to dryness. Then, the mixture was placed into a furnace and heated up to 500 °C at a rate of 250 °C/hour. The calcination was completed at 500 °C for the next 1 hour before further cooling to room temperature overnight. The product of the synthesis was washed 6 times with demineralized water on a centrifuge. Finally, the powder was dried in air at 90 °C.

TaC supported electrocatalysts were prepared with concentrations of 10, 30, 50, 70, 90 and 100 wt.% of IrO_2 and labelled as $(IrO_2)_x(TaC)_{1-x}$, where x is the mass fraction of IrO_2. Si_3N_4 support samples with 30, 50, 70, 90 and 100 wt.% of IrO_2 were prepared and labeled similarly. Additionally, the Adams fusion process was also applied to pure TaC to see the impact of the synthesis conditions on the support properties.

Physico-chemical characterisation

Thermogravimmetric and differential thermal analysis. The supports were investigated using DTA/TGA analysis (Netzsch STA 409 PC) with a heating rate of 5 °C/min and a maximum temperature of 400 °C and 1000 °C for Si_3N_4 and TaC respectively (Figure 1). Si_3N_4 exhibited great stability over the temperature range with a slight weight loss ascribed to loss of surface-bound compounds. A transformation of TaC to Ta_2O_5 was seen over the temperature range. This reaction accelerated at 600 °C. At 330 °C, well below the temperature of the Adams fusion, 1 wt.% was converted and we can safely assume, that at 790 °C the whole sample had been turned into Ta_2O_5.
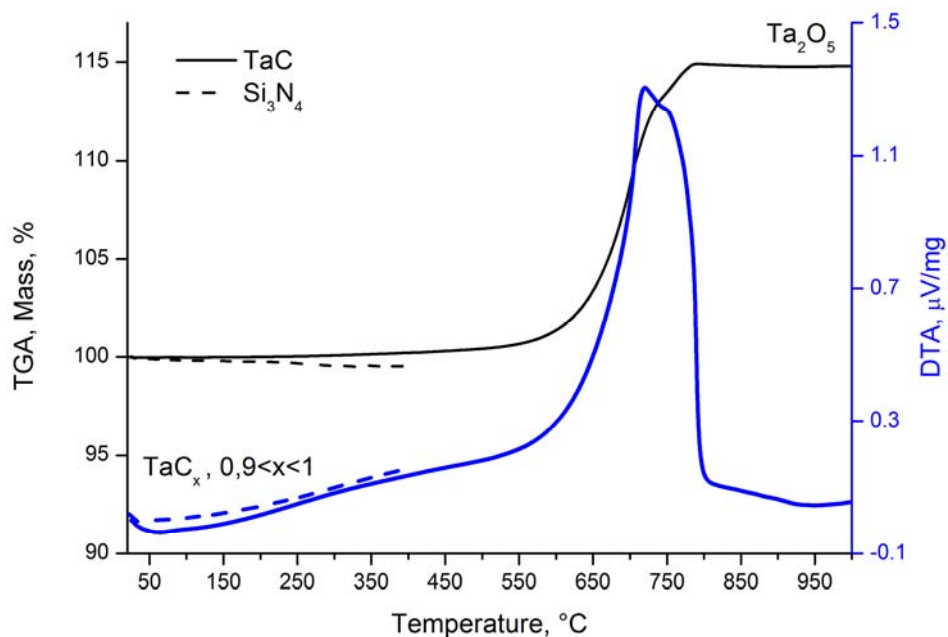
Figure 1. Thermogravimmetric (thin line) and differential thermal analysis (thick line) curves of TaC and Si_3N_4 in synthetic air. Heating rate 5 °C/min. Data for TaC is published as (2).
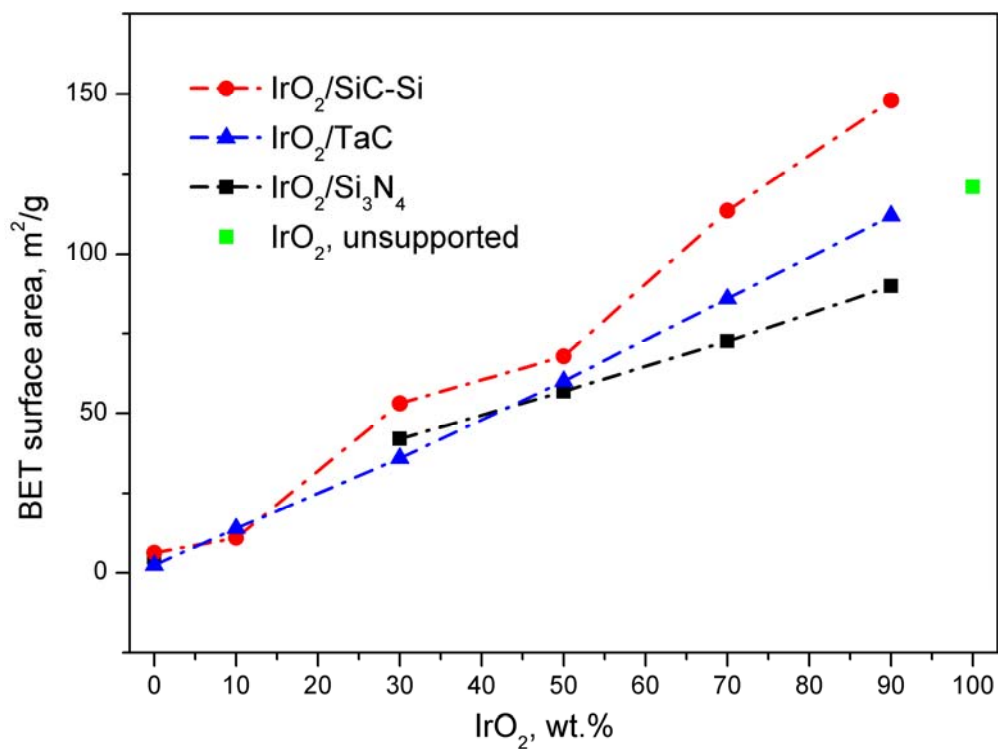

Figure 2. BET surface area of the prepared electrocatalysts. Data for IrO_2/SiC-Si and IrO_2/TaC is published as (1) and (2) respectively.

117

BET. Specific surface area (SSA) of the electrocatalyst and also the as-received supports was calculated from N_2 adsorption performed using a Micromeritics Gemini 2375 analyser. The results are shown in Figure 2 together with previously published data for IrO_2/SiC-Si and IrO_2/TaC (1,2). It is seen that, contrary to what was seen for SiC-Si, there is no gain in SSA by introduction of any of the two other supports. While the SSA of the IrO_2/TaC electrocatalysts corresponds to a linear combination of the SSA of IrO_2 and TaC respectively, Si_3N_4 promotes a decrease in SSA compared to the weighted contribution of IrO_2.
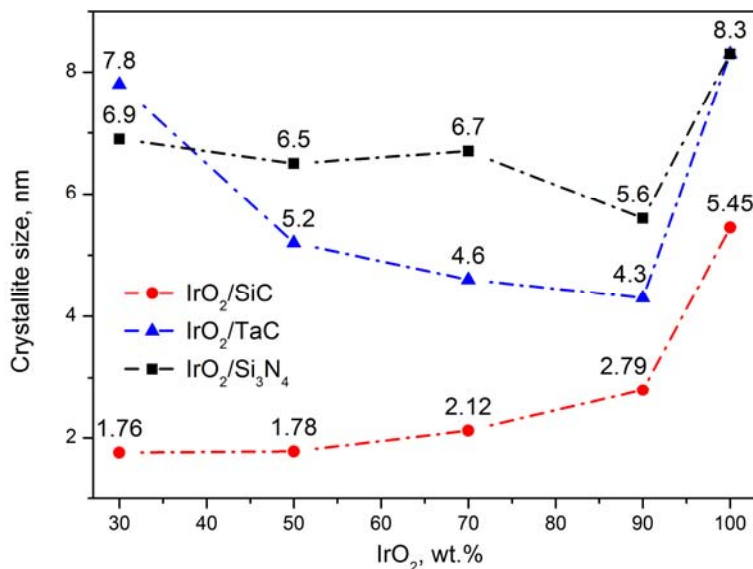

Figure 3. IrO_2 crystallite size calculated by the Scherrer equation from XRD powder diffraction. Data for IrO_2/SiC-Si and IrO_2/TaC is published as (1) and (2) correspondingly.

XRD. X-ray powder diffraction was done using a Huber D670 diffractometer (Cu-Kα, α = 1.5405981 Å). Figure 3 depicts a plot of crystallite size, calculated on the basis of the Scherrer equation for different types of electrocatalysts. Addition of support lowers the crystallite size for all supported catalysts. For Si_3N_4 this effect is most profound at the addition of 10 wt.% support and a stabilisation of the effect is seen for larger amount of support. TaC shows a similar minima in crystallite size at 10 wt.% support but does not stabilise and rises to a crystallite size very close to pure IrO_2 at 70 wt.% support. This may be explained by the decrease of the number of available nucleation centres because the concentration of the precursor drops with increased ratio of the support.

It can be seen from comparison of Figure 2 and Figure 3, that, unlike IrO_2/SiC-Si, decrease in IrO_2 crystallite size on Si_3N_4 and TaC supports is not followed by the increase of the catalyst SSA. Therefore, there is no direct connection between the crystallite size and SSA for these two materials.
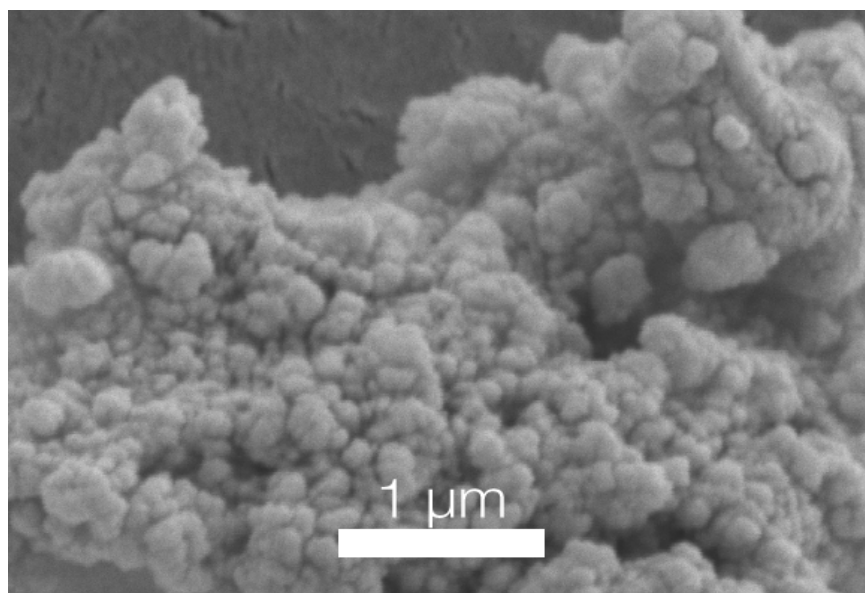
Figure 4. SEM image of 50 wt.% TaC electrocatalyst. Secondary electron detector used.
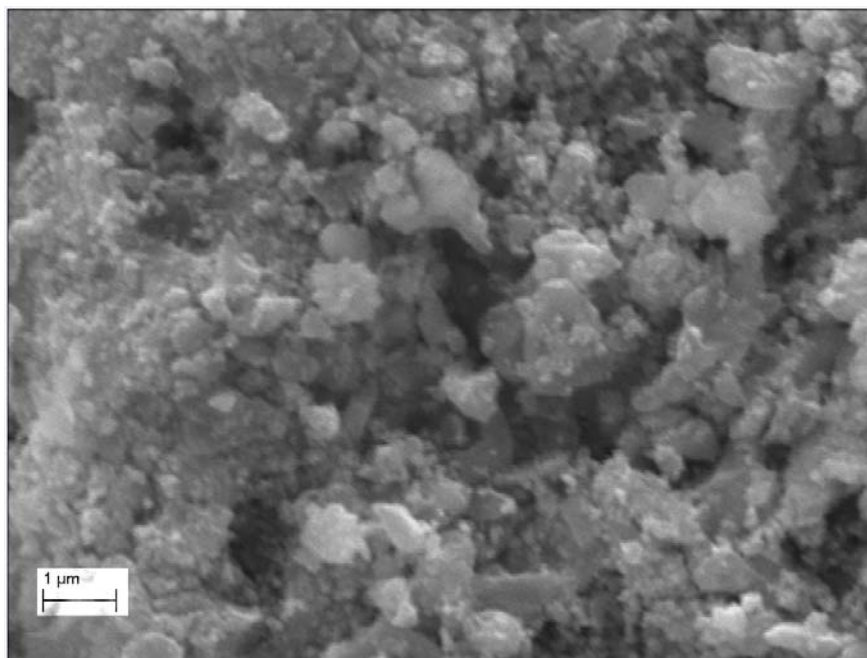

Figure 5. SEM image of 50 wt.% Si_3N_4 electrocatalyst. Secondary electron detector used.

SEM. To investigate the morphology of the electrocatalysts SEM imaging was carried out using a Zeiss Evo MA 10 microscope. The TaC supported compounds (Figure 4) showed, similar to the SiC-Si electrocatalysts (1), nano-size spherical agglomerations of IrO_2 stabilised on support particles. This is the desired shape as the high surface-to-mass ratio inherited from the spherical form facilitates high electrocatalytic activity.

The Si_3N_4 supported samples (Figure 5) showed a rugged and edgy geometry and imaging with back-scattering electron detection visualised it being Si_3N_4 particles coated with a layer of IrO_2. This clarified the loss of SSA, seen in Figure 2, with the addition of

Si$_3$N$_4$ as support since the normal spherical agglomeration is disrupted as it is more energetically favourable for IrO$_2$ to cover Si$_3$N$_4$.
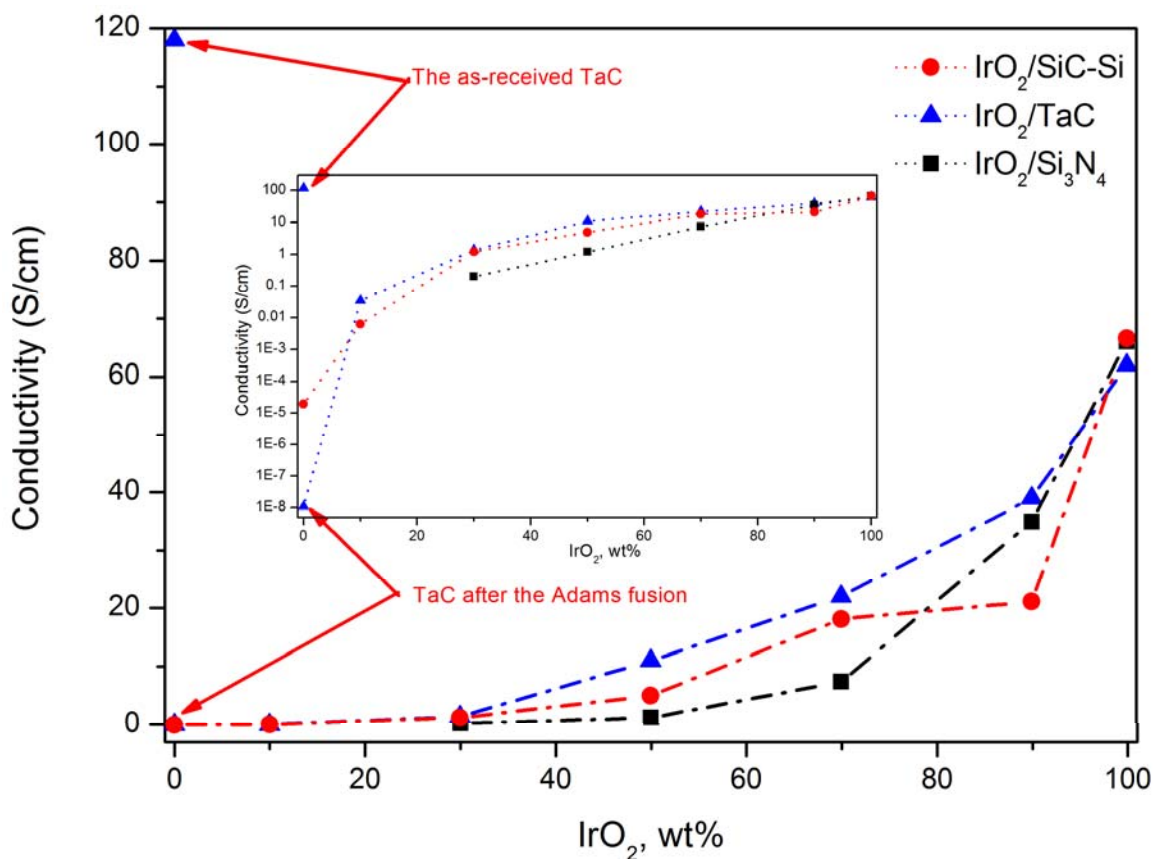

Figure 6. Powder conductivity measurements of TaC, Si$_3$N$_4$ and SiC-Si respectively.

Powder conductivity. Figure 6 depicts the results of powder conductivity measurements of the produced electrocatalysts as well as for the as-received supports and for a TaC sample, which has been subjected to the same conditions as during the Adams fusion to see the effect of the process on the powder conductivity. It can be seen that TaC gets passivated with the surface oxide, which was shown earlier by the TGA/DTA data.

Development of conductivity of TaC powder, subjected to heating in air at 84 °C and 150 °C at different length of time is presented in Figure 7. It can be outlined that at temperature 84 °C there is no appreciable loss in conductivity with time. However, at 150 °C the oxidation of the TaC surface is more pronounced and the conductivity levels-off after the treatment in hot air for approximately 800 hours. The achieved values of conductivity after 800 hours, corresponding to approximately 10 S/cm is still high for the electrocatalytic layer (4). The results also suggest that the chosen Adams fusion process for the supported catalyst was not the optimal choice in this case and if the temperature of synthesis is lowered from 500 °C to e.g. 150 °C, the conductivity of the TaC support can be considerably improved in the final electrocatalyst.
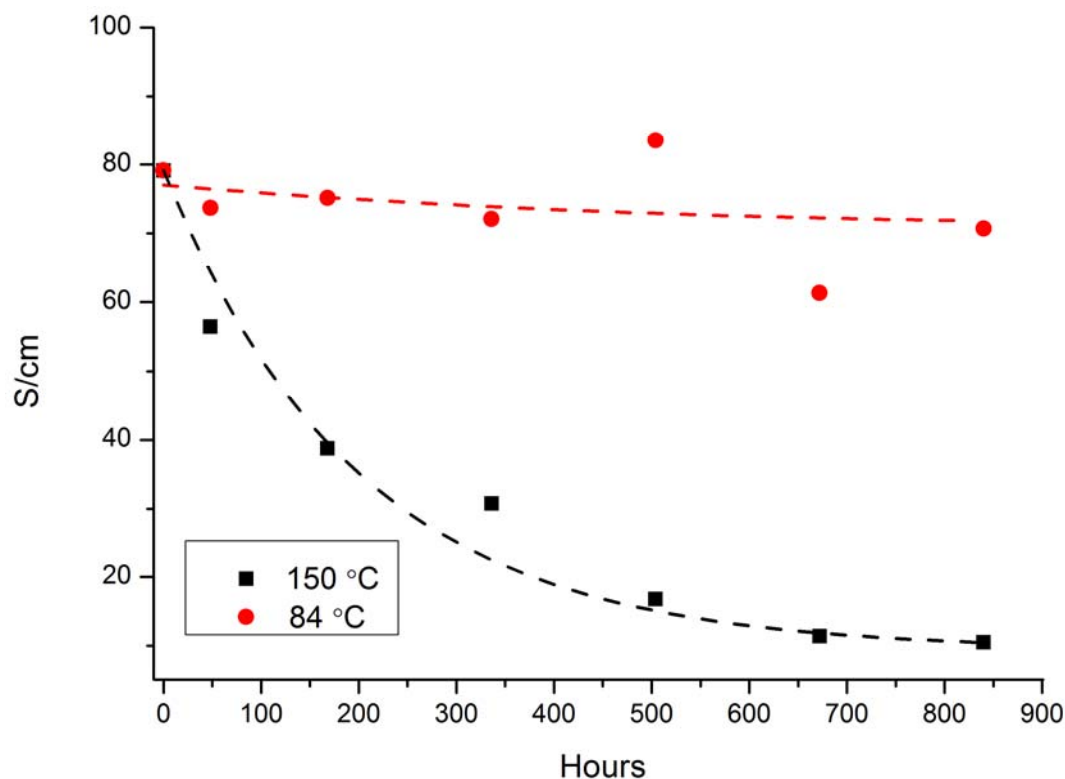
Figure 7. Powder conductivity of TaC, after different time of exposure to atmosphere at 84 and 150 °C.

Not surprisingly, the Si_3N_4 supported sample showed the lowest conductivity. This originates from the insulating nature of Si_3N_4, which means that the support will under no circumstance contribute to the conductivity. Furthermore, the coating of the Si_3N_4 particles seen by SEM may result in bad contact between the particles and to be a factor, contributing to the low conductivity. Even though the electrocatalysts with the semi-conducting supports showed better performance, it was not significantly better. The 90 wt.% IrO_2 sample with the semi-conducting SiC-Si support even performs worse than the corresponding Si_3N_4 sample.
Even the worst performing sample from 50 wt.% IrO_2 and up performs well enough for further investigation in a MEA as it can be calculated that conductivity of ≥ 1 S/cm will not lead to significant ohmic losses in the PEMWE.

Electrochemical characterization

Cyclic voltammetry. Cyclic voltammogramms in all the experiments corresponded to the behavior of IrO_2 electrocatalysts, reported previously (5). The shape is characterized by a broad redox peak, located at approximately 0.9 V vs. SCE and corresponding to the total number of active sites (6). As it can be found in Figure 8, in the potential region between 0.4 and 1.2 V vs. SCE, the anodic and cathodic parts of the voltammogramm present quite high degree of reversibility. Generally, for investigation of such system, the reversibility value of Q_a/Q_c can be implemented to assess the contribution of the second component in the mixed electrocatalyst, as the Q_a/Q_c ratio is expected to be close to unity (7). Figure 9 represents the summarized results of the Q_a/Q_c ratio vs. the composition of

the TaC-supported electrocatalysts. The charges were integrated using a scan rate of 500 mV/s in the potential region between 0.4 and 1.2 V vs. SCE. The ratio for the TaC-supported electrocatalysts with ≥ 50 wt.% IrO_2 was close to unity and increased with the increasing loading of the support, indicating worse support surface coverage by IrO_2 and more pronounced interaction of the support with the electrolyte. However, for Si_3N_4 support, the behavior was quite different, showing higher values of the Q_a/Q_c ratio. As the values for the pure IrO_2 powder differ significantly with the similar experiments for TaC series. It was explained by the different type of the glassy carbon electrodes used in the series and therefore the direct comparison of electrochemical results for the different supports is not possible. However, comparing the relative change of Q_a/Q_c values, depending on the IrO_2 loading, it is clear that the dependence is less pronounced than for a TaC sample (Figure 10). It was attributed to a different type of surface interaction between IrO_2 and Si_3N_4 support, probably connected with better surface adhesion of active electrocatalyst to the support. The confirmation of SEM images on Figures 4, 5 can confirm this hypothesis. It also suggests that in case of using Si_3N_4 as a catalyst support, its surface gets coated with a compact layer of IrO_2 and further increase of the loading of the active electrocatalyst does not change the Q_a/Q_c parameter, which suggests that the active surface of the electrode has the same morphology independent of IrO_2 loading. This behaviour corresponds to the development of calculated BET surface area for IrO_2/Si_3N_4 supported electrocatalysts, which decreased with introduction of the support and was lower than expected from the weighted contribution of IrO_2. However, stability of the supported electrocatalysts appears to be independent on the IrO_2 loading.

Conclusions

In this study it was shown that the crystallite size was smaller in the presence of support for all the supports tested. However, the influence of support on the overall electronic conductivity of the electrocatalysts was negative. SEM images revealed that the formation of IrO_2 particles is different in the presence of different supports, which influences the morphology of the electrode. That was also confirmed by the CV results, where no considerable interaction between the surfaces of the support and electrocatalyst was observed in the case of Si_3N_4. On the other hand, the behavior of TaC supported electrocatalysts becomes more reversible with increasing portion of IrO_2 in the composite.

Acknowledgements
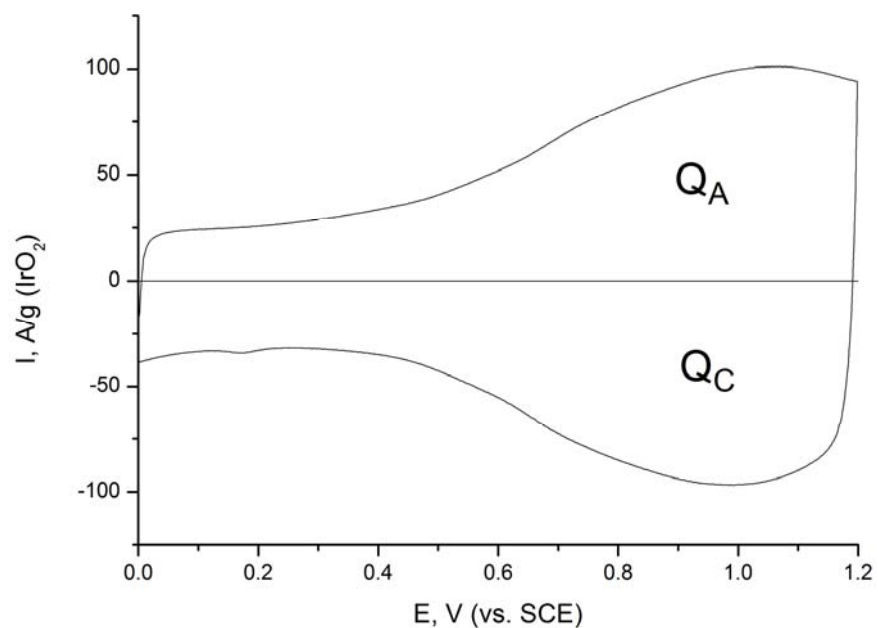
Figure 8. Cyclic voltammogram of a $(IrO_2)_{0.5}(TaC)_{0.5}$ sample. Potential sweep rate 500 mV/s, 0.5M H_2SO_4, room temperature.
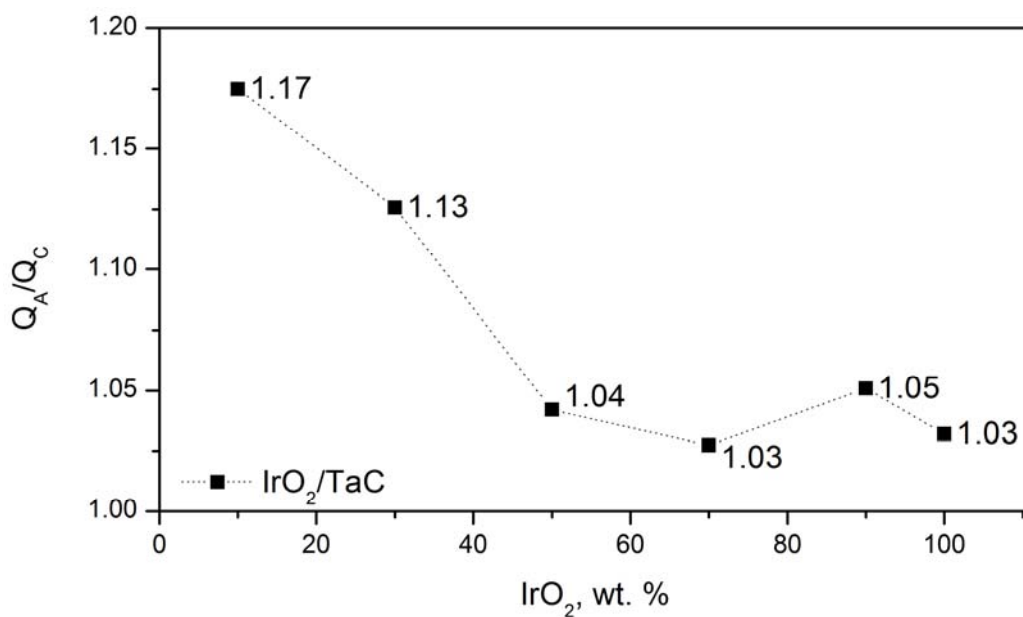
Figure 9. Ratio of anodic-to-cathodic charge for a IrO_2/TaC supported electrocatalyst. Charge is integrated between 0.4 and 1.2 V. Potential sweep rate 500 mV/s, 0.5M H_2SO_4, room temperature.
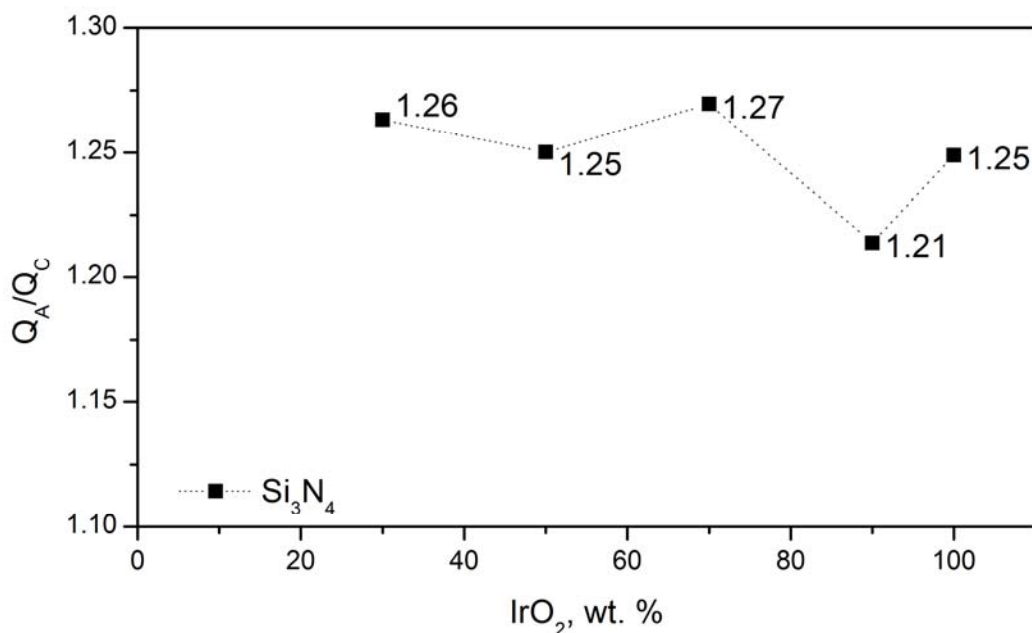
Figure 10.   Ratio of anodic-to-cathodic charge for a IrO_2/Si_3N_4 supported electrocatalyst. Charge is integrated between 0.4 and 1.2 V. Potential sweep rate 500 mV/s, 0.5M H_2SO_4, room temperature.

References

1. A.V. Nikiforov, A.L. Tomás-García, I.M. Petrushina, E. Christensen and N.J. Bjerrum, *Int J Hydrogen Energy*, **36(10)**, 5797 (2011).
2. J. Polonský, I.M. Petrushina, E. Christensen, K.Bouzek, C.B. Prag, J.E.T. Andersen and N.J. Bjerrum, *Int J Hydrogen Energy*, accepted (2011)
3. W. Martienssen, H. Warlimon, editors. *Springler Handbook of Condensed Matter and Materials Data*, Springer, Berlin (2005).
4. S. Trasatti, *J. Electrochim Acta*, **36(2)**, 225-241 (2010).
5. A. T. Marshall, R.G. Hoverkamp, *J. Electrochim Acta*, **55**, 1978-1984 (2010).
6. C. Comninellis, G.P. Vercesi., *J. Appl Electrochem*, **21**, 335-345 (1991).
7. C.P. De Pauli, S. Trasatti, *J. Electroanal Chem,* **396**, 161-168 (1995).